Am J Physiol Heart Circ Physiol 283: H1099–H1107, 2002.
First published May 23, 2002; 10.1152/ajpheart.00270.2002.

Microvascular reperfusion injury: rapid expansion of anatomic no reflow during reperfusion in the rabbit

THORSTEN REFFELMANN AND ROBERT A. KLONER
The Heart Institute, Good Samaritan Hospital, University of Southern California, Los Angeles, California 90017-2395

Received 28 March 2002; accepted in final form 2 May 2002

Reffelmann, Thorsten, and Robert A. Kloner. Microvascular reperfusion injury: rapid expansion of anatomic no reflow during reperfusion in the rabbit. *Am J Physiol Heart Circ Physiol* 283: H1099–H1107, 2002. First published May 23, 2002; 10.1152/ajpheart.00270.2002.—The aim was to define the degree and time course of reperfusion-related expansion of no reflow. In five groups of anesthetized, open-chest rabbits (30-min coronary occlusion and different durations of reperfusion), anatomic no reflow was determined by injection of thioflavin S at the end of reperfusion and compared with regional myocardial blood flow (RMBF; radioactive microspheres) and infarct size (triphenyltetrazolium). The area of no reflow progressively increased from 12.2 ± 4.2% of the risk area after 2 min of reperfusion to 30.8 ± 3.1% after 2 h and 34.9 ± 3.3% after 8 h and significantly correlated with infarct size after 1 h of reperfusion (r = 0.88–0.97). This rapid expansion of no reflow predominantly occurred during the first 2 h, finally encompassing ~80% of the infarct size, and was accompanied by a decrease of RMBF within the risk area, being hyperemic after 2 min of reperfusion (3.78 ± 0.75 $ml \cdot min^{-1} \cdot g^{-1}$) and plateauing at a level of ~0.9 $ml \cdot min^{-1} \cdot g^{-1}$ by 2 and 8 h of reperfusion (preischemic RMBF: 2.06 ± 0.01 $ml \cdot min^{-1} \cdot g^{-1}$). The development of macroscopic hemorrhage lagged behind no reflow, was closely correlated with it, and may be the consequence of microvascular damage.

myocardial infarction; microcirculation; vasculature; hemorrhage

MICROVASCULAR DAMAGE after reperfusion therapy for acute myocardial infarction may limit the completeness of tissue perfusion despite reopening of the epicardial vessel. This "no-reflow" phenomenon, which was first observed in animal studies of coronary occlusion and reperfusion, has been characterized by decreased resting myocardial blood flow, distinct areas of hypoperfusion, and functional vascular damage within the previously ischemic tissue (1, 22, 30).

Because reperfusion therapy has become one of the pivotal goals in acute myocardial infarction, the no-reflow phenomenon has obtained increasing attention in clinical situations. The significance of no reflow for predicting clinical outcome, myocardial viability, and contractile recovery, as well as treatment strategies to prevent no reflow, is being evaluated in several studies, using myocardial contrast echocardiography, angiographic parameters, and magnetic resonance imaging (9, 13, 17, 18, 26, 28, 32, 34, 35).

However, microvascular damage may depend to a substantial degree on reperfusion injury. As demonstrated in a canine model by Ambrosio et al. (1), perfusion defects increased more than twofold between 2 min and 3.5 h of reperfusion. Since then, evidence for a progression of no reflow with ongoing reperfusion emerged even in the clinical situation of reperfused acute myocardial infarction (17, 18, 19, 23). However, the exact time course of progression of anatomic no reflow during reperfusion is not well defined, both in experimental animal designs and clinical circumstances (29).

Thus we sought to define the development of anatomic no reflow within the first 8 h of reperfusion in a rabbit model of coronary occlusion and reperfusion to achieve insight into the degree and time course of microvascular reperfusion injury.

METHODS

The experiments were conducted in accordance with the national and institutional Guide for the Care and Use of Laboratory Animals.

Animal Preparation

New Zealand White male rabbits (2.0–3.2 kg) were anesthetized by intramuscular ketamine (400 mg) and xylazine (200 mg). After tracheotomy, ventilation was initiated by means of a mechanical respirator (model 665, Harvard Apparatus Respirator; South Natick, MA) using room air enriched with 1.5 l/min oxygen. Fluid-filled catheters were inserted into the right jugular vein and carotid artery for additional anesthesia (pentobarbital, as needed to suppress the blinking reflex) and continuous monitoring of arterial blood pressure.

After a left lateral thoracotomy in the fourth intercostal space and pericardial incision, a major branch of the circumflex coronary artery was encircled by a suture (4-0 silk suture, Ethicon; Sommerville, NJ). By threading the two ends of the suture through a piece of plastic tubing, a snare was formed, which could be tightened to achieve coronary artery occlusion. A fluid-filled catheter was inserted into the left atrial appendage and

Address for reprint requests and other correspondence: R. A. Kloner, The Heart Institute, Good Samaritan Hospital, Univ. of Southern California, 1225 Wilshire Blvd., Los Angeles, CA 90017-2395 (E-mail: RKloner@goodsam.org).

The costs of publication of this article were defrayed in part by the payment of page charges. The article must therefore be hereby marked "*advertisement*" in accordance with 18 U.S.C. Section 1734 solely to indicate this fact.

fixed by a clip. Rectal temperature was monitored, and a heating pad was used to maintain body temperature.

Hemodynamics

Heart rate and systolic and diastolic blood pressure were measured and averaged over three consecutive cardiac cycles for each sample period. Variations in heart rate and blood pressure over these three cycles were minimal (<5 beats/min and <5 mmHg, respectively).

Assessment of Ischemic Risk Area, Area of No Reflow, and Infarct Size

At the end of the protocol, 1 ml/kg of 4% thioflavin S [dissolved in 0.9% saline and then centrifuged (1,500 rpm) for 5 min, Sigma; St Louis, MO] was injected into the left atrium. Thioflavin S is a vital fluorescent stain for endothelium. After ~1 min, the coronary artery was reoccluded and 4 ml of 50% Uniperse blue (Ciba Geigy; Hawthorne, NY) was injected into the left atrium to measure the ischemic risk area. The rabbits were euthanized by an intravenous overdose of xylazine (100 mg) followed by 12 meq intra-atrial potassium chloride. After removal of the heart, the left ventricle was sliced into five to seven transverse sections. The slices were photographed under water, rephotographed under ultraviolet light in a dark room (365-nm wave length, Spectroline model ENF 280 C, Spectronics; Westbury, NY) using a Y48 barrier filter (Minolta), and again photographed after incubation in 1% triphenyltetrazolium chloride (TTC; 37°C, for ~15 min). TTC stains viable myocardium red; necrotic tissue appears pale yellow. The contour of each slice; the risk area (not stained by the blue dye); the macroscopic hemorrhage, visible as brownish-red tissue within the risk area; the area of no reflow (ANR), defined as the nonfluorescent area; and the area not stained by TTC were traced manually from the projected slides. No staining technique was used to visualize the hemorrhagic tissue, which was obvious by inspection of the heart slices as dark reddish-brown areas. After computerized planimetry, the percentage of the areas was multiplied by the weight of the slice. The risk area was expressed as a percentage of the weight of the left ventricle; the hemorrhage, the ANR, and the TTC-negative area were expressed as a percentage of the weight of the risk area.

Regional Myocardial Blood Flow

Regional myocardial blood flow (RMBF) was measured by intra-atrial injection of ~500,000 microspheres per measurement, labeled with ^{96}Nb, ^{141}Ce, or ^{103}Ru. Simultaneously, a reference blood sample was withdrawn through the arterial catheter at a rate of 2.06 ml/min. The hearts were cut into samples stained by the blue dye (nonischemic tissue) and not stained by the dye (tissue at risk). Great effort was used in carefully dissecting the entire risk area for the assessment of RMBF, thus representing an average of the whole risk area. Tissue and blood sample radioactivity was counted using a multichannel pulse-height analyzer (model ND62, Nuclear Data; Schaumburg, IL). RMBF was calculated after correction for background and crossover as the ratio of counts in the tissue and the reference blood sample multiplied by the reference flow rate and divided by the weight of the tissue sample.

Protocols

Protocol 1: main study. All of the animals were subjected to 30 min of coronary artery occlusion, followed by reperfusion for either 2, 30, 60, 120, or 480 min (*groups I–V*, $n = 9$ animals/group). RMBF was measured at different time points (Table 1). When RMBF was measured at the end of the protocol, intra-atrial injection of the microspheres was begun 1 min before the injection of thioflavin S. In one heart, data on hemorrhage were not available due to technical reasons.

Protocol 2: sham animals. To assess the influence of anesthesia, surgery, and instrumentation of the heart, in particular with respect to the long duration of anesthesia in *group V*, two animals were anesthetized and instrumented in the same way except that the snare was not tightened. RMBF was determined at baseline, 150 min, and 510 min before thioflavin S was injected into the left atrium, and the animals were euthanized.

Statistical Analysis

Data are expressed as means ± SE. The area at risk, ANR, the area not stained by TTC, and the hemorrhage in the groups of the main study were compared by one-way ANOVA with subsequent Tukey's post hoc test. Trend analysis between these parameters and reperfusion time in these five groups was performed using a linear regression model. The RMBF data during reperfusion, measured at two time points in the course of reperfusion in *groups II–V*, were compared using a paired Student's *t*-test in each group. A P value of <0.05 was considered statistically significant.

RESULTS

Hemodynamics

Coronary artery occlusion was followed by a marked decrease of systolic and diastolic blood pressure and an increase in heart rate in the five groups (Fig. 1). During reperfusion, systolic and diastolic blood pressure tended to further decrease, which was accompanied by an increase in heart rate. Temperature was relatively stable during the protocols. Six rabbits assigned to *group V* and one rabbit assigned to *group IV*, which died during reperfusion because of progressive hypotension, were excluded from the analysis and replaced.

The time course of hemodynamics in the sham animals, which showed a similar decrease of blood pressure (Table 2), suggests that the decrease in blood pressure during reperfusion could mainly be attributed to the effect of anesthesia and opening of the chest.

Infarct Size

The average risk area in the five groups ranged between 30.1% and 32.0%. The area not stained by

Table 1. *Experimental protocol in the five groups of the main study*

Group	Occlusion, min	Reperfusion, min	RMBF, time points
I	30	2	Baseline, 15-min occlusion, 2-min reperfusion
II	30	30	Baseline, 2-min reperfusion, 30-min reperfusion
III	30	60	Baseline, 30-min reperfusion, 60-min reperfusion
IV	30	120	Baseline, 60-min reperfusion, 120-min reperfusion
V	30	480	Baseline, 120-min reperfusion, 480-min reperfusion

$n = 9$ animals/group. RMBF, regional myocardial blood flow.

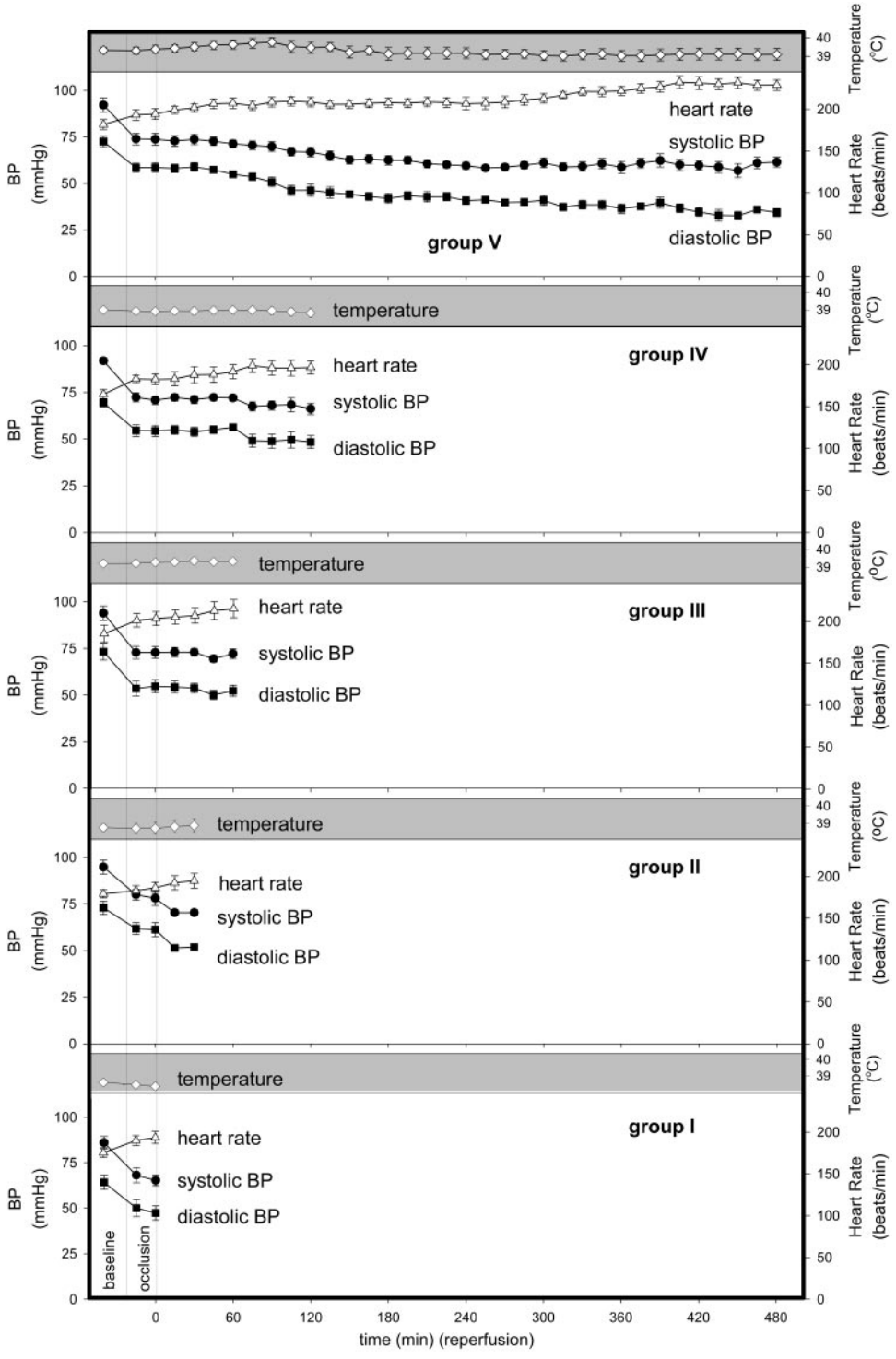

Fig. 1. Hemodynamics and rectal temperature in the 5 groups. BP, blood pressure.

TTC was significantly smaller in *groups I* and *II* compared with *group V* (Fig. 2). Infarct size in *group V* amounted to 44.1 ± 3.8% and was not significantly different from infarct size in *groups III* and *IV* (37.7 ± 3.6% and 37.1 ± 2.5%). The potential limitations of TTC staining for the assessment of infarct size with short periods of reperfusion are discussed below. However, because the TTC-negative area in *groups III* and *IV* did not significantly differ from that of *group V*, these values may serve as a good estimate for infarct size in these groups.

ANR and Hemorrhage

The ANR was below 10% of the risk area in six of nine animals in *group I* (Figs. 2 and 3). However, three hearts showed a substantial perfusion defect, even after 2 min of reperfusion. The average ANR was

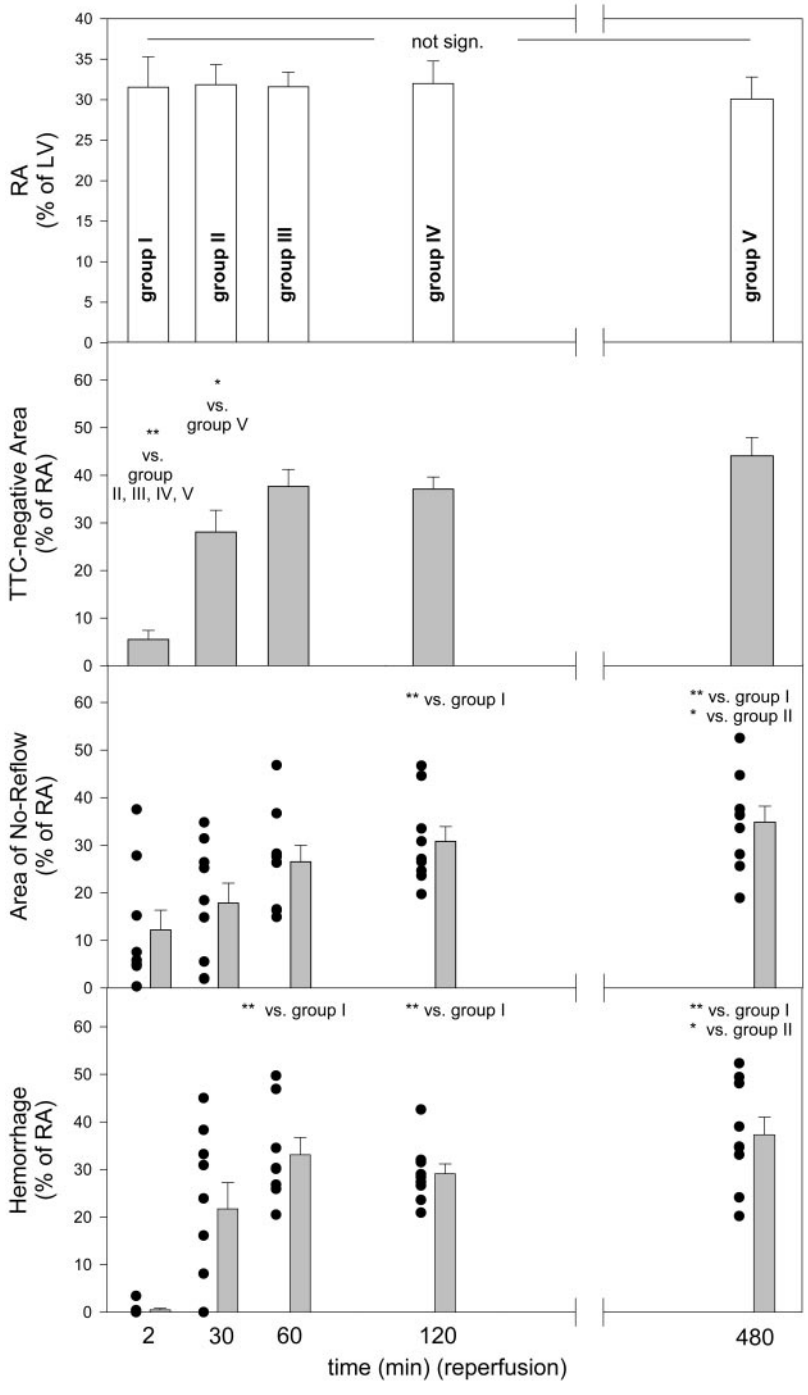

Fig. 2. Risk area (RA), triphenyltetrazolium chloride (TTC), area of no reflow (ANR), and macroscopic hemorrhage in the 5 groups. LV, left ventricle; sign, significant. $*P < 0.05$; $**P < 0.01$.

12.2 ± 4.2% of the risk area in *group I*, which was significantly smaller than that in *groups IV* and *V*. There was a progressive increase of anatomic no reflow in the groups with longer reperfusion times, and the ANR as a percentage of the risk area was 30.8 ± 3.1% after 2 h of reperfusion (*group IV*) and 34.9 ± 3.3% after 8 h of reperfusion (*group V*) (82.4 ± 4.2% and 79.4 ± 4.2% of the infarct size, respectively). The increase in anatomic no reflow mainly occurred within the first 2 h of reperfusion, with only a little increase between 2 and 8 h of reperfusion. With the use of a linear regression model, a significant trend toward larger ANRs with longer reperfusion time was apparent ($P < 0.0007$). The ANR in *groups III–V* was always smaller than the TTC-negative area, and the size of the ANR significantly correlated with the amount of necrosis in these groups ($r = 0.88–0.97$).

The amount and spatial distribution of the macroscopic hemorrhage closely correlated with the ANR in *groups II–V* ($r = 0.72–0.95$). After 2 min of reperfusion, essentially no hemorrhage was visible except for minor spots adjacent to the suture. However, the hemor-

rhagic tissue increased with ongoing reperfusion and reached a value of 37.3 ± 3.7% of the risk area in *group V*. Again, a significant trend toward increasing size of the hemorrhage with longer reperfusion was obvious ($P < 0.0004$).

In contrast, the two sham animals revealed a homogenous distribution of fluorescence after 8.5 h without occlusion except a small nonfluorescent area with hemorrhage at the site of the suture in one animal.

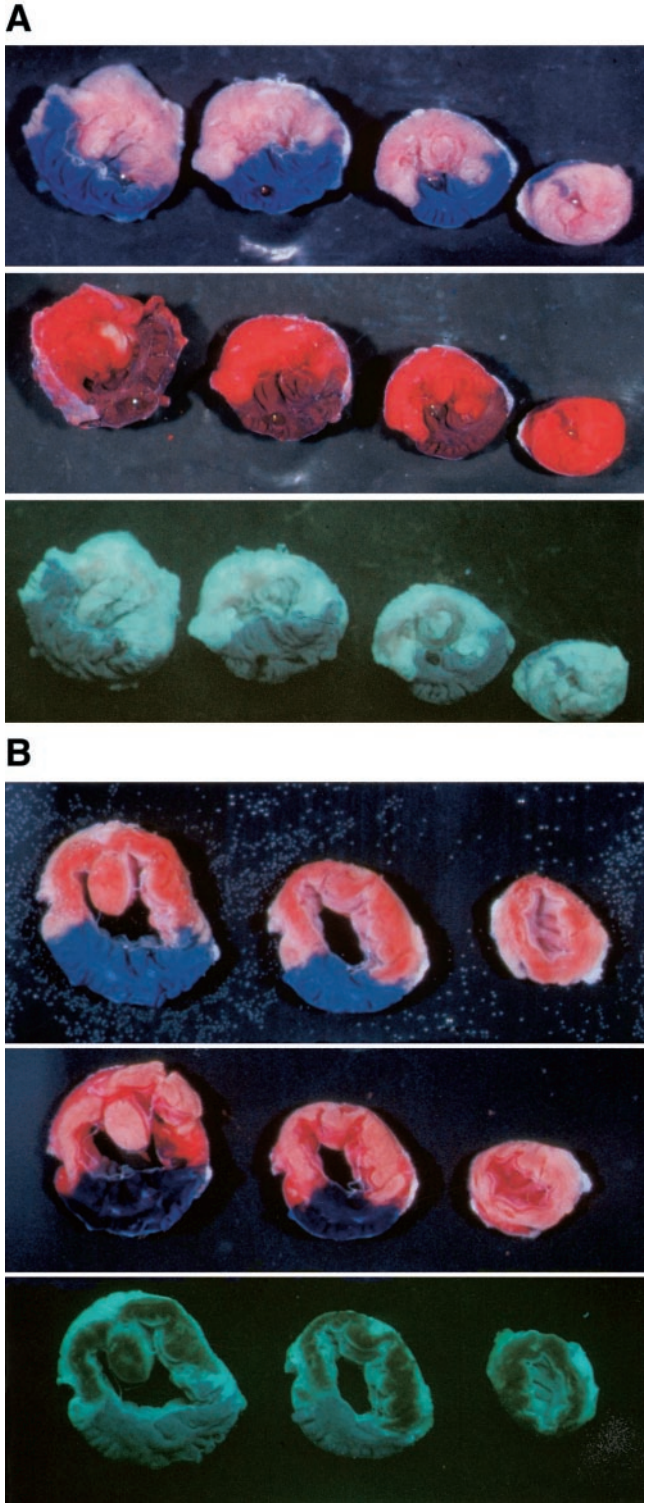

Fig. 3. Apical slices of hearts after 30 min of occlusion and 2 min of reperfusion (*A*) and 8 h of reperfusion (*B*). *A*: after 2 min of reperfusion, there is no macroscopically visible hemorrhage in the risk area (*top*), the TTC-negative area is relatively small (*middle*), and only small zones within the risk area appear nonfluorescent under an ultraviolet light (*bottom*). *B*: after 8 h of reperfusion, however, the risk area contains a substantial amount of brownish-red tissue, defined as the macroscopic hemorrhage (*top*). TTC staining leaves the necrotic tissue unstained, showing a pale white to yellow color after 8 h of reperfusion (*middle*). Sizable nonfluorescent zones, the area of no reflow, are visible after 8 h, which closely correlates with hemorrhage and necrosis (*bottom*). Within the nonischemic tissue, less fluorescence is visible due to the blue dye.

Regional Myocardial Blood Flow

RMBF at baseline ranged between 1.76 ± 0.13 and 2.44 ± 0.19 $ml \cdot min^{-1} \cdot g^{-1}$ in nonischemic tissue (Fig. 4). RMBF in the risk area during occlusion was 0.02 ± 0.01 $ml \cdot min^{-1} \cdot g^{-1}$ in *group I*, i.e., negligible collateral flow. During reperfusion, RMBF in the risk area was hyperemic with 2 min of reperfusion and then progressively declined during reperfusion. After 2 h of reperfusion, RMBF within the risk area seemed to reach a plateau at a level of ~0.90 $ml \cdot min^{-1} \cdot g^{-1}$. Correlation analysis of RMBF in the risk area at the end of the experiment versus size of anatomic no reflow revealed an inverse correlation in each group ($r = -0.50$ to -0.75, $P < 0.02$–0.18).

In the nonischemic tissue, RMBF did not significantly change during the course of the experiments, but RMBF at 8 h of reperfusion was substantially but not significantly increased.

The data of the sham animals (Table 2) suggest that this increase might be most likely related to changes of whole body physiology by anesthesia, open-chest, and instrumentation.

DISCUSSION

The main results of this study are as follows: *1*) Anatomic no reflow increases nearly threefold between 2 min and 8 h of reperfusion. *2*) The most significant portion of this increase occurs during the first hour and to a lesser extent during the second hour of reperfusion. *3*) After initial hyperemic reflow, RMBF in the risk area rapidly declines and reaches a plateau at ~0.9 $ml \cdot min^{-1} \cdot g^{-1}$ with 2 and 8 h of reperfusion, which is ~50% of normal nonischemic flow. *4*) The development of macroscopic hemorrhage lags behind the development of anatomic no reflow but correlates well with its extent and spatial distribution after 30 min of reperfusion. Thus it appears to be the consequence of microvascular injury.

Thioflavin S as a Marker of No Reflow

In several studies, the technique of thioflavin S staining to delineate anatomic no reflow was shown to be highly accurate when compared against ultrastructural signs of microvascular damage and compared

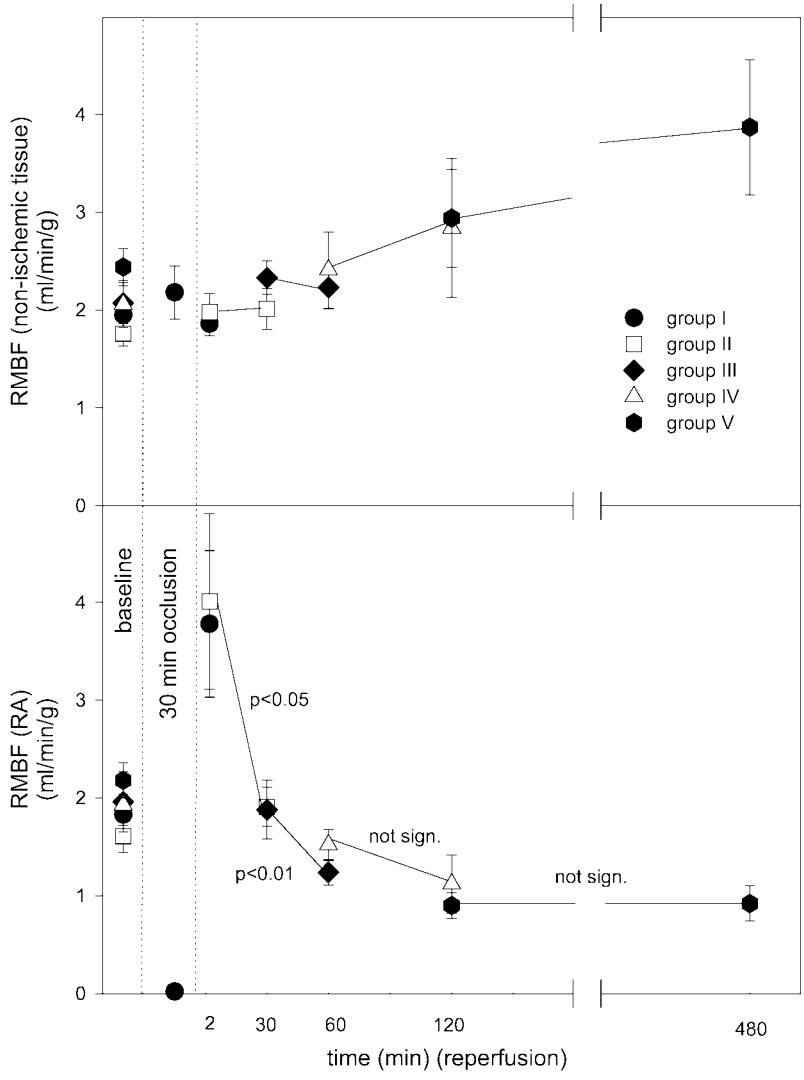

Fig. 4. Regional myocardial blood flow (RMBF) in nonischemic tissue (*top*) and within the RA (*bottom*) for the 5 groups.

with other dyes (e.g., carbon black) used to stain reperfused tissue (22). In the canine model, areas of nonfluorescence after thioflavin S were characterized by a RMBF of <50% of normal flow, both after short and long durations of reperfusion (1). Autofluorescence of heart slices (without thioflavin S staining), as demonstrated in some pilot experiments, was mainly confined to connective tissue and the endo- and epicardial surface. To further validate this technique in the rabbit, we compared the size of nonfluorescent areas and zones not stained by the blue dye 50% Uniperse blue, which was injected simultaneously with thioflavin S at the end of the experiment without reocclusion, in nine different experiments with durations of occlusion between 30 and 120 min and durations of reperfusion between 2 and 120 min. Size and spatial distribution of no-reflow zones closely correlated with each other (r = 0.98). Interestingly, the areas not stained by the blue dye, which is a suspension of blue particles, were always slightly larger than the nonfluorescent areas [ANR (percentage of the left ventricle, thioflavin S) = −0.4 + 0.8 ANR (percentage of the left ventricle, blue dye)]. This might indicate that anatomic no reflow is a gradual phenomenon with small border zones of re-

Table 2. *Hemodynamics in two sham animals (protocol 2)*

	Baseline	30 min	150 min	270 min	390 min	510 min
Systolic BP, mmHg	95 ± 2	89 ± 2	81 ± 9	67 ± 1	57 ± 4	62 ± 6
Diastolic BP, mmHg	75 ± 3	66 ± 4	55 ± 7	44 ± 2	32 ± 2	30 ± 1
Heart rate, beats/min	205 ± 12	248 ± 31	209 ± 14	203 ± 18	236 ± 6	251 ± 14
RMBF, ml·min^{-1}·g^{-1}	1.62 ± 0.55		2.52 ± 0.29			4.11 (n = 1)

Values are means ± SE; n = no. of animals. BP, blood pressure.

duced flow that are stained or not, depending on the ability of the specific dye to penetrate into these zones of low reflow. In addition, this relationship may reflect the ability of the eye to discriminate between stained and nonstained tissue, depending on the color of the used dye.

Thus this technique appears to be appropriate in this model. Furthermore, the accuracy was not influenced by the duration of occlusion or reperfusion.

Time Course of Microvascular Reperfusion Injury

Most animal studies that addressed the issue of microvascular reperfusion injury were performed in a canine model of coronary occlusion and reperfusion. One of the first fundamental investigations by Ambrosio et al. (1) found an increase in the ANR, visualized by thioflavin S, from 9.5% at 2 min of reperfusion to 25.9% of the risk area at 3.5 h of reperfusion. Interestingly, these zones of no reflow were characterized by nearly no collateral blood flow during occlusion. However, the exact time course of anatomic no reflow during reperfusion has not been clarified for years except for these two time points at 2 min and 3.5 h of reperfusion (29).

The data of the present study in the rabbit model, which is characterized by negligible collateral blood flow, extend the findings by Ambrosio et al. (1) by defining the time course and degree of this expansion of microvascular damage during reperfusion: The major part of reperfusion-related increase in anatomic no reflow occurs within the first hour of reperfusion, with markedly less progression within the second hour, and only a minimal, if any, increase between 2 and 8 h of reperfusion. RMBF, assessed as an average of the whole risk area, parallels this time course of anatomic no reflow, reaching a plateau at 2 h of reperfusion. Within the foci of no reflow, however, RMBF can be assumed to be markedly lower. In addition, RMBF in the risk area closely correlated with the size of no reflow in each group.

A recent study by Rochitte et al. (31) used hypoenhancement visible after contrast enhancement on magnetic resonance imaging as a measure of microvascular obstruction in reperfused canine infarcts. In contrast to our findings, they reported a progressive increase of microvascular obstruction from 2 h (13%) to 6 h (23%) of reperfusion and a further growth by 48 h of reperfusion (30% of infarct size). One might speculate that these differences are solely species related, because the rabbit model, in contrast to the canine model, is subjected to more severe and uniform ischemia during occlusion due to its negligible collateral flow. However, hypoenhancement on magnetic resonance imaging and zones of nonfluorescence after thioflavin S may also substantially differ from each other and may be differently influenced by the duration of reperfusion. Despite a strong correlation between hypoenhancement and thioflavin S negative areas after 2 days of reperfusion, only ~50% of the thioflavin S-negative area in this study by Rochitte et al. (31) and ~25% in a comparable study (21) demonstrated hypoenhancement on magnetic resonance imaging.

With the use of scintigraphic techniques, Jeremy et al. (20) convincingly demonstrated reperfusion-related worsening of tissue perfusion in the canine model as well. In this study, tissue perfusion, assessed by ^{82}Ru-positron emission tomography, declined within the first 4 h of reperfusion (20).

The time course of reperfusion-related expansion of no reflow in clinical situations is even less well defined. Characteristic changes of intravascular flow velocity patterns, assessed by intravascular Doppler measurements, were observed in the first 10 min after interventional recanalization for acute myocardial infarction (19). Assessment of coronary venous flow demonstrated a progressive decrease in the first 24 h after reperfusion therapy for acute anterior wall infarction (23). Asanuma et al. (2) found a new contrast defect on myocardial contrast echocardiography in 25% of patients with anterior myocardial infarction after 31 days compared with contrast echocardiography shortly after reopening of the epicardial artery.

Mechanisms of No Reflow

Although many different concepts have been developed to explain the occurrence of the no-reflow phenomenon, their significance and mutual interrelations are not yet clarified (for a review, see Ref. 30).

Localized endothelial swelling and membrane-bound intraluminal bodies are the major ultrastructural characteristics of the microvascular bed after temporary ischemia that may directly contribute to compromised tissue perfusion, probably early after reflow (22). Oxygen-derived free radicals (5, 27) and leukocyte accumulation (6, 7, 11) during reperfusion are regarded as crucial mechanisms in the progression of no reflow during reperfusion. The rapid expansion of the no-reflow zone in the present study apparently supports this concept. Tissue edema has also been put forward to explain microvascular hypoperfusion by mechanical compression (24). However, this probably cannot explain the worsening of myocardial blood flow within the first 2 h of reperfusion, because tissue edema in general develops very rapidly after reflow. In the present study, baseline RMBF in the risk area, measured at the end of the protocol, was slightly lower than RMBF in the nonischemic tissue in every group, most likely due to the development of edema during reperfusion. Thus baseline RMBF in the risk zone, expressed as a percentage of baseline RMBF in the nonischemic myocardial tissue, may serve as an estimate for the amount of tissue edema that has developed during reperfusion. Apparent baseline RMBF in the risk area amounted to 93 ± 5% of RMBF in the nonischemic tissue already after 2 min of reperfusion and did not further decrease during this period of rapid expansion of no reflow (92 ± 6% after 1 h of reperfusion and 95 ± 6% after 2 h of reperfusion) nor did this percentage significantly correlate with the ANR ($P < 0.20$), which does not support

a major role of tissue edema in the observed progression of no-reflow zones.

Spasm of resistance vessels has also been put forward to explain the marked reduction of tissue perfusion after myocardial infarction (14, 15). The mutual interrelations between morphological signs of endothelial damage and a potential contribution of precapillary spasm to the perfusion defects remain to be determined.

Coagulation and thrombotic microvascular occlusion are not believed to play a primary role in the development of no reflow. However, as recently demonstrated in the rabbit, tissue factor might be involved in no reflow by activating factor VII when exposed to flowing blood (12). In the clinical setting of acute myocardial infarction, coronary microembolization from disrupted plaques or thrombotic lesions significantly contributes to microvascular damage, which is not simulated in most animal models of coronary occlusion and reperfusion (30, 33).

Hemorrhage and Microvascular Injury

The rabbit heart, a model without relevant collateral flow, is apparently very prone to the development of hemorrhage during reperfusion. While there was nearly no macroscopically visible hemorrhage after 2 min of reperfusion, the amount of hemorrhage in the other groups closely correlated with the ANR. As demonstrated by Higginson et al. (16), hemorrhage in the canine model predominantly occurred in myocardial tissue that had obtained nearly no collateral flow during coronary occlusion and was confined to areas of myocardial necrosis. Fishbein et al. (10) suggested that hemorrhage was a consequence of preexisting vascular injury and not its cause, which is in accordance with our observation that the development of hemorrhage lagged behind the occurrence of ANR. Even a recent clinical study (2) using magnetic resonance imaging for detection of intramyocardial hemorrhage and myocardial contrast echocardiography for detection of perfusion defects demonstrated that intramyocardial hemorrhage only occurred in patients with sizable contrast defects.

Limitations

The TTC staining with short durations of reperfusion remains inconclusive. According to Birnbaum et al. (4), infarct size, as assessed by TTC staining in a similar animal model, seemed to reach a plateau by 2–3 h of reperfusion but was significantly smaller with shorter durations of reperfusion (4), which is in accordance with the findings of the present study. However, whether reflecting the ability of TTC to adequately stain necrotic tissue, or a true progression of necrosis during reperfusion, cannot be clarified by the present study (3, 8, 25).

In addition, we have to reckon with substantial changes in whole body physiology due to open-chest and anesthesia, in particular in the long reperfusion group, as suggested by the decreased blood pressure and increased RMBF in the sham group. We cannot exclude that resting RMBF in the risk area after 8 h of reperfusion is even more compromised than our data suggest, which might be measured under a hyperemic stimulus.

However, it seems to be unlikely that the amount of anatomic no reflow is significantly influenced by blood pressure at the end of the experiment, when thioflavin S was given, as the high RMBF in the nonischemic tissue (*group V*) demonstrates that compromised tissue perfusion is not due to hypotension. In addition, blood pressure at the end of the protocol and the size of the ANR were not inversely correlated, both when all individual animals of the main study were analyzed together ($r = -0.15$) and for separate analyses in each group.

Summary and Conclusions

Reperfusion injury appears to be responsible for a nearly threefold increase of anatomic no reflow within the first 8 h of reperfusion accompanied by a parallel decrease of RMBF. This expansion of no reflow predominantly occurs during the first 2 h of reperfusion, finally encompassing ~80% of the infarct. The development of macroscopic hemorrhage lags behind no reflow and seems to be the consequence of microvascular injury.

This study was supported in part by the Joseph Drown Foundation and National Heart, Lung, and Blood Institute Grant HL-61488.

This study was presented in part as an abstract on the 51st scientific session of the American College of Cardiology, Atlanta, 2002.

REFERENCES

1. **Ambrosio G, Weisman HF, Mannisi JA, and Becker LC.** Progressive impairment of regional myocardial perfusion after initial restoration of postischemic blood flow. *Circulation* 80: 1846–1861, 1989.
2. **Asanuma T, Tanabe K, Ochiai K, Yoshitomi H, Nakamura K, Murakami Y, Sano K, Shimada T, Murakami R, Morioka S, and Beppu S.** Relationship between progressive microvascular damage and intramyocardial hemorrhage in patients with reperfused anterior myocardial infarction. *Circulation* 96: 448–453, 1997.
3. **Becker LC, Jeremy RW, Schaper J, and Schaper W.** Ultrastructural assessment of myocardial necrosis occurring during ischemia and 3-h reperfusion in the dog. *Am J Physiol Heart Circ Physiol* 277: H243–H252, 1999.
4. **Birnbaum Y, Hale SL, and Kloner RA.** Differences in reperfusion length following 30 minutes of ischemia in the rabbit influence infarct size, as measured by triphenyltetrazolium chloride staining. *J Mol Cell Cardiol* 29: 657–666, 1997.
5. **Duilio C, Ambrosio G, Kuppusamy P, DiPaula A, Becker LC, and Zweier JL.** Neutrophils are the primary source of O_2 radicals during reperfusion after prolonged myocardial ischemia. *Am J Physiol Heart Circ Physiol* 280: H2649–H2657, 2001.
6. **Engler RL, Dahlgren MD, Peterson MA, Dobbs A, and Schmid-Schonbein GW.** Accumulation of polymorphonuclear leukocytes during 3-h experimental myocardial ischemia. *Am J Physiol Heart Circ Physiol* 251: H93–H100, 1986.
7. **Engler RL, Schmid-Schonbein GW, and Pavelec RS.** Leukocyte capillary plugging in myocardial ischemia and reperfusion in the dog. *Am J Pathol* 111: 98–111, 1983.
8. **Farb A, Kolodgie FD, Jenkins M, and Virmani R.** Myocardial infarct extension during reperfusion after coronary artery occlusion: pathologic evidence. *J Am Coll Cardiol* 21: 1245–1253, 1993.

9. **Fisher NG, Leong-Poi H, Sakuma T, Rim SJ, Bin JP, and Kaul S.** Detection of coronary stenosis and myocardial viability using a single intravenous bolus injection of BR14. *J Am Coll Cardiol* 39: 523–529, 2002.
10. **Fishbein MC, Y-Rit J, Lando U, Kanmatsuse K, Mercier JC, and Ganz W.** The relationship of vascular injury and myocardial hemorrhage to necrosis after reperfusion. *Circulation* 62: 1274–1279, 1980.
11. **Go LO, Murry CE, Richard VJ, Weischedel GR, Jennings RB, and Reimer KA.** Myocardial neutrophil accumulation during reperfusion after reversible or irreversible ischemic injury. *Am J Physiol Heart Circ Physiol* 255: H1188–H1198, 1988.
12. **Golino P, Ragni M, Cirillo P, Scognamiglio A, Ravera A, Buono C, Guarino A, Piro O, Lambiase C, Botticella F, Ezban M, Condorelli M, and Chiarello M.** Recombinant human, active site-blocked factor VIIa reduces infarct size and no-reflow phenomenon in rabbits. *Am J Physiol Heart Circ Physiol* 278: H1507–H1516, 2000.
13. **Grube E, Gerckens U, Yeung AC, Rowold S, Kirchhof N, Sedgewick J, Yadav JS, and Stertzer S.** Prevention of distal embolization during coronary angioplasty in saphenous vein grafts and native vessels using porous filter protection. *Circulation* 104: 2436–2441, 2001.
14. **Hellstrom RH.** Coronary artery stasis after induced myocardial infarction in the dog. *Cardiovasc Res* 5: 371–375, 1971.
15. **Hellstrom RH.** Evidence in support of the spasm of resistance vessel concept of ischemic heart disease: an update in 1993. *Med Hypotheses* 41: 11–22, 1993.
16. **Higginson LA, White F, Heggtveit HA, Sanders TM, Bloor CM, and Covell JW.** Determinants of myocardial hemorrhage after coronary reperfusion in the anesthetized dog. *Circulation* 65: 62–69, 1982.
17. **Ito H, Iwakura K, Oh H, Masuyama T, Hori M, Higashino Y, Fujii K, and Minamino T.** Temporal changes in myocardial perfusion patterns in patients with reperfused anterior wall myocardial infarction. Their relation to myocardial viability. *Circulation* 91: 656–662, 1995.
18. **Ito H, Okamura A, Iwakura K, Masuyama T, Hori M, Takiuchi S, Negoro S, Nakatsuchi Y, Taniyama Y, Higashino Y, Fujii K, and Minamino T.** Myocardial perfusion patterns related to thrombolysis in myocardial infarction perfusion grades after coronary angioplasty in patients with acute anterior wall myocardial infarction. *Circulation* 93: 1993–1999, 1996.
19. **Iwakura K, Ito H, Nishikawa N, Hiraoka K, Sugimoto K, Higashino Y, Masuyama T, Hori M, Fujii K, and Minamino T.** Early temporal changes in coronary flow velocity patterns in patients with acute myocardial infarction demonstrating the "no-reflow" phenomenon. *Am J Cardiol* 84: 415–419, 1999.
20. **Jeremy RW, Links JM, and Becker LC.** Progressive failure of coronary flow during reperfusion of myocardial infarction: documentation of the no reflow phenomenon with positron emission tomography. *J Am Coll Cardiol* 16: 695–704, 1990.
21. **Judd RM, Lugo-Olivieri CH, Arai M, Kondo T, Croisille P, Lima JA, Mohan V, Becker LC, and Zerhouni EA.** Physiological basis of myocardial contrast enhancement in fast magnetic resonance images of 2-day-old reperfused canine infarcts. *Circulation* 92: 1902–1910, 1995.
22. **Kloner RA, Ganote CE, and Jennings RB.** The "no-reflow" phenomenon after temporary coronary occlusion in the dog. *J Clin Invest* 54: 1496–1508, 1974.
23. **Komamura K, Kitakaze M, Nishida K, Naka M, Tamai J, Uematzu M, Koretsune Y, Nanto S, Hori M, Inoue M, Kamada T, and Kodama K.** Progressive decreases in coronary vein flow during reperfusion in acute myocardial infarction: clinical documentation of the no reflow phenomenon after successful thrombolysis. *J Am Coll Cardiol* 24: 370–377, 1994.
24. **Manciet LH, Poole DC, McDonagh PF, Copeland JG, and Matthieu-Costello O.** Microvascular compression during myocardial ischemia: mechanistic basis for no-reflow phenomenon. *Am J Physiol Heart Circ Physiol* 266: H1541–H1550, 1994.
25. **Matsumura K, Jeremy RW, Schaper J, and Becker LC.** Progression of myocardial necrosis during reperfusion of ischemic myocardium. *Circulation* 97: 795–804, 1998.
26. **Morishima I, Sone T, Okumara K, Tsuboi H, Kondo J, Mukawa H, Matsui H, Toki Y, Ito T, and Hayakawa T.** Angiographic no-reflow as a predictor of adverse long-term outcoume in patients treated with percutaneous transluminal coronary angioplasty for first myocardial infarction. *J Am Coll Cardiol* 36: 1202–1209, 2000.
27. **Przyklenk K and Kloner RA.** "Reperfusion injury" by oxygen-derived free radicals? Effect of superoxide dismutase plus catalase, given at the time of reperfusion, on myocardial infarct size, contractile function, coronary microvasculature, and regional myocardial blood flow. *Circ Res* 64: 86–96, 1989.
28. **Ragosta M, Camarano G, Kaul S, Powers ER, Sarembock IJ, and Gimple LW.** Microvascular integrity indicates myocellular viability in patients with recent myocardial infarction. New insights using myocardial contrast echocardiography. *Circulation* 89: 2562–2569, 1994.
29. **Reffelmann T, Hale SL, Li G, and Kloner RA.** Relationship between no reflow and infarct size as influenced by the duration of ischemia and reperfusion. *Am J Physiol Heart Circ Physiol* 282: H766–H772, 2002.
30. **Reffelmann T and Kloner RA.** The "no-reflow" phenomenon: basic science and clinical correlates. *Heart* 87: 162–168, 2002.
31. **Rochitte CE, Lima JA, Bluemke DA, Reeder SB, McVeigh ER, Furuta T, Becker LC, and Melin JA.** Magnitude and time course of microvascular obstruction and tissue injury after acute myocardial infarction. *Circulation* 98: 1006–1014, 1998.
32. **Sakuma T, Otsuka M, Okimoto T, Fujiwara H, Sumii K, Imazu M, and Hayashi Y.** Optimal time for predicting myocardial viability after successful primary angioplasty in acute myocardial infarction: a study using myocardial contrast echocardiography. *Am J Cardiol* 87: 687–692, 2001.
33. **Topol EJ and Yadav JS.** Recognition of the importance of embolization in artherosclerotic vascular disease. *Circulation* 101: 570–580, 2000.
34. **Villanueva FS, Glasheen WP, Sklenar J, and Kaul S.** Assessment of risk area during coronary occlusion and infarct size after reperfusion with myocardial contrast echocardiography using left and right atrial injections of contrast. *Circulation* 88: 596–604, 1993.
35. **Wu KC, Zerhouni EA, Judd RM, Lugo-Olivieri CH, Barouch LA, Schulman SP, Blumenthal RS, and Lima JAC.** Prognostic significance of microvascular obstruction by magnetic resonance imaging in patients with acute myocardial infarction. *Circulation* 97: 765–772, 1998.